Electronic Supplementary Information for

Effect of Tight Flavin Mononucleotide Wrapping and its Binding Affinity on Carbon Nanotube Covalent Reactivities

Jinsook Sim, Hyunkyu Oh, Eunhye Koo, and Sang-Yong Ju[*]

Department of Chemistry, Yonsei University, Seoul 120-749, South Korea

* Correspondence E-mail: syju@yonsei.ac.kr

Methods for Normalization of Absorption Spectra. Figure 3A shows the as-obtained absorbance spectra. To determine the reactivity of 4-methoxybenzenediazonium tetrafluoroborate (4-MBD) towards nanotube sidewalls, we subtracted the background contributed by nanotube bundling and carbonaceous impurities by drawing a straight line between the troughs of each absorption band as described in a previously published paper.[S1] Troughs were taken at 550, 588, 628, 715, 787, 855, 921, 1041, 1079, 1107, 1190, 1247, and 1350 nm. The results are shown in Fig. S1. The initial and consequent time-dependent heights were used as denominators and numerators, respectively, to calculate the normalized absorption ratio of E_{11}^{M} metallic (560 and 600 nm) and E_{22}^{S} semiconducting (659, 743, 813, and 874 nm) SWNT transitions. Due to the significantly large water absorption at 956, 1222, and 1410 nm (shown in Fig. S1), we used photoluminescence intensity to determine the diazonium salt reaction kinetics of E_{11}^{S} semiconducting SWNTs.

Detailed Method of XPS Characterization. Further information about degree of functionalization can be obtained from an analysis of X-ray photoelectron spectroscopy (XPS). XPS data of before and after covalent functionalization samples are illustrated in Figure S2. XPS data from both samples showed that repeated mild sonication/decantation cycles still left small amount of FMN on SWNTs sidewalls, judging from N1s peaks. N atomic contents were 2.2 and 5.2 % for before and after the covalent functionalization. Considering atomic contents of FMN, we subtract a FMN contribution from total amount of carbon and oxygen contents. The results are listed in Table S3. The determined oxygen contents before and after functionalization were 5.4% and 5.6%, respectively. About 0.2% of oxygen, originating from 4-MBD, was excess in covalently-functionalized sample with 4-MBD. Inset shows XPS spectra of C1*s* (left) and O1*s* (right). XPS spectrum of C1s from both before and after functionalization shows sp^2 hybridized carbon at 284.6eV, originating from sp^2 hybridized carbon. Peaks from sp^3 carbon at 285.2eV significantly increased after functionalization, indicating the successful covalent functionalization.

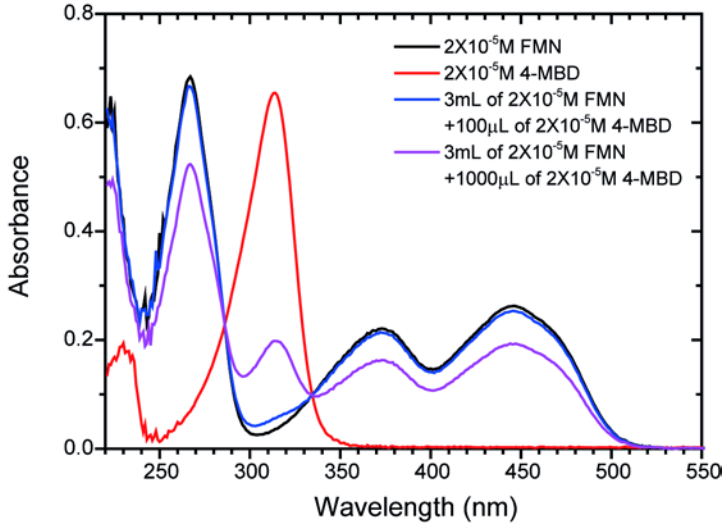

Fig. S1. Absorption spectra of 2×10^{-5} M FMN (black), 2×10^{-5} M 4-MBD (red), and 3 mL of 2×10^{-5} M FMN in the presence of 100 μL (blue) and 1000 μL (magenta) of 2×10^{-5} M 4-MBD.

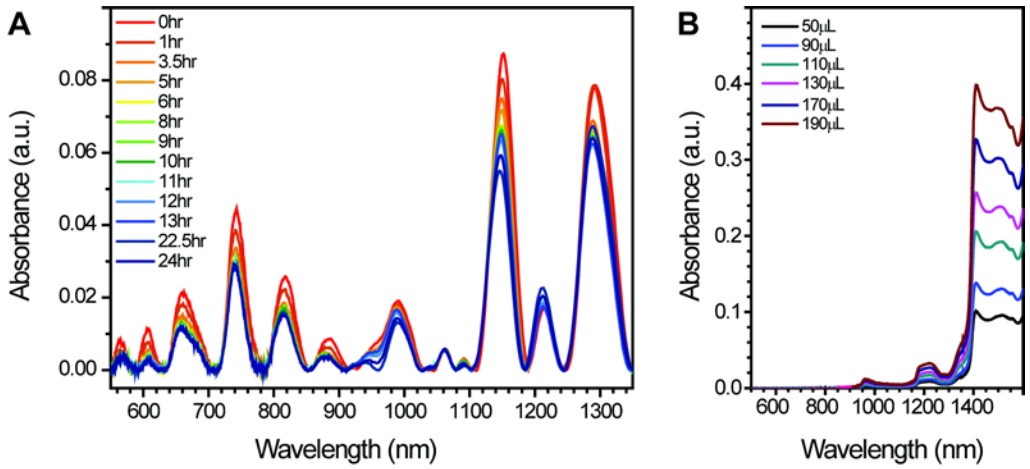

Fig. S2. (A) Background-subtracted absorption spectra of FMN-SWNT from Fig. 3A. (B) Absorption spectra of H_2O titrated against 3 mL D_2O.

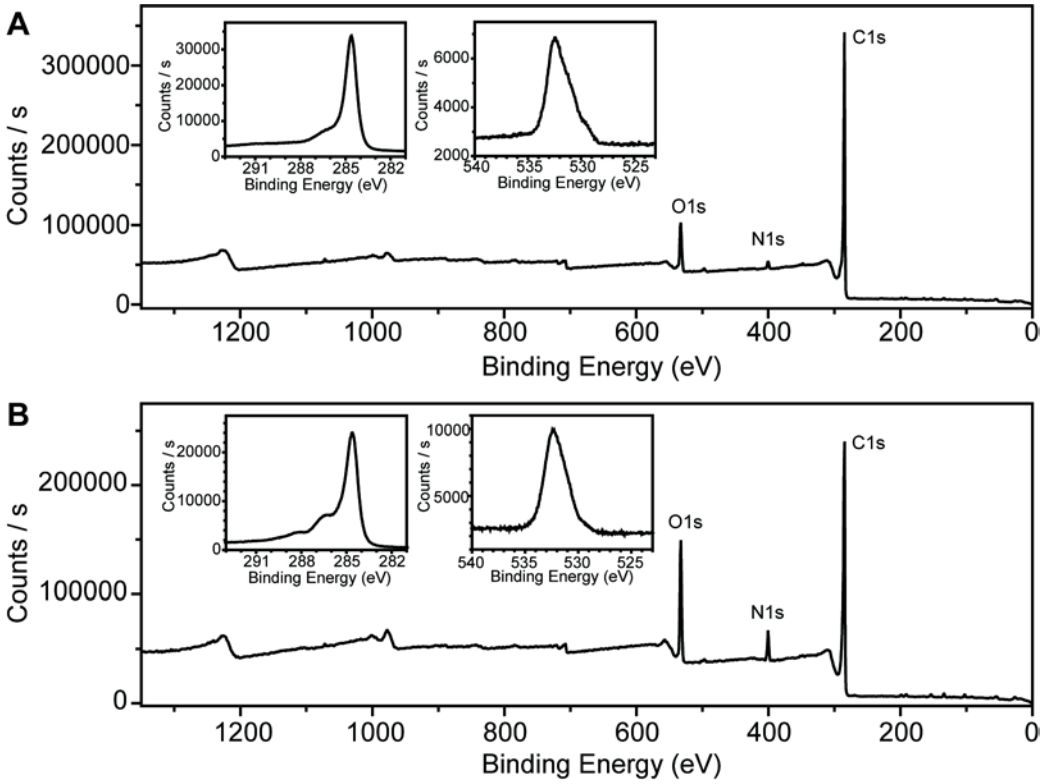

Fig. S3. X-ray photoelectron spectra (XPS) of FMN-SWNTs (A) without and (B) with covalent functionalization.Inset shows XPS spectra from C1*s* (left) and O1*s* (right).

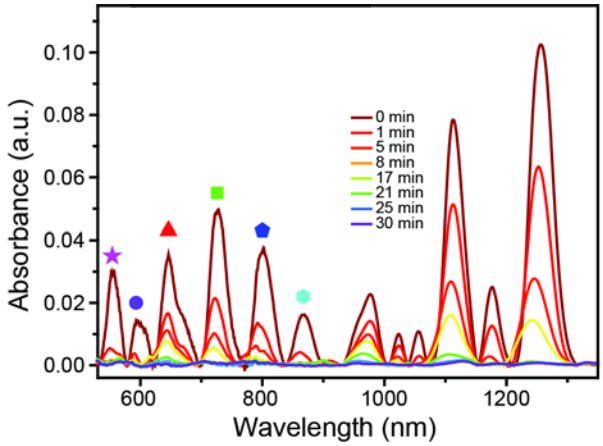

Fig. S4. Background-subtracted absorption spectra of SDS-SWNT from Figure 4A.

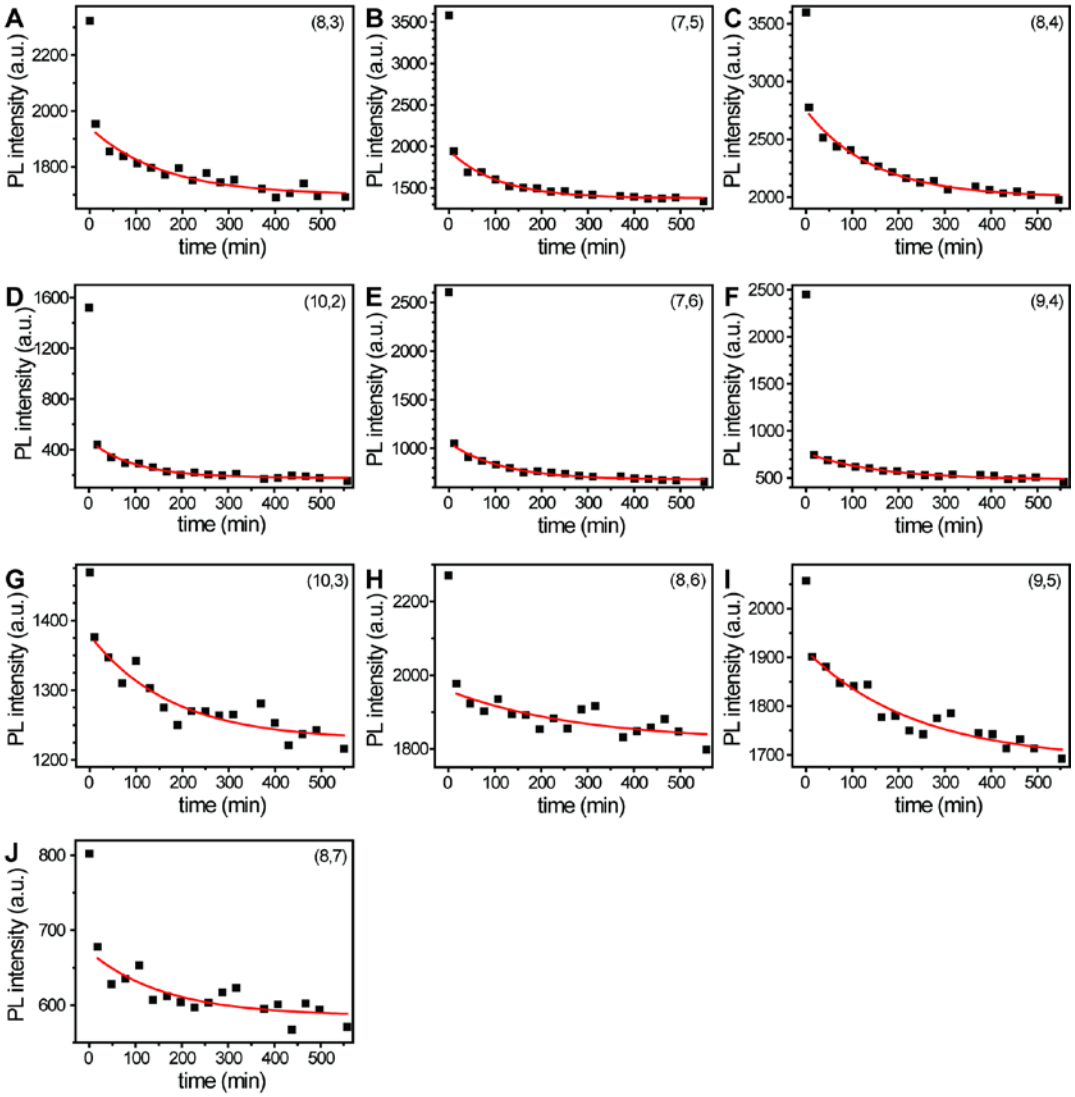

Fig. S5. Photoluminescence decay kinetics of nanotubes modified by diazonium reagent according to nanotube chiralities. Data were fitted using an exponential decay curve (in red).

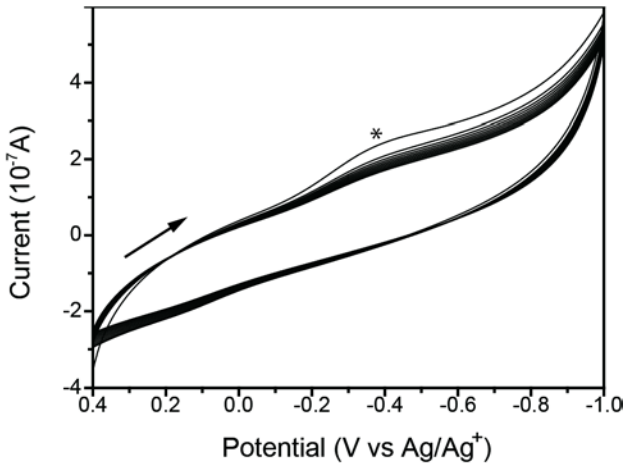

Fig. S6. Cyclovoltamogram of 4-MBD measured in acetonitrile. Reference electrode was Ag/Ag$^+$. Voltage was swapped from -1.0 V to 0.4 V with scan speed was 20 mV/s. Asterisk indicates the reduction potential of 4-MBD.

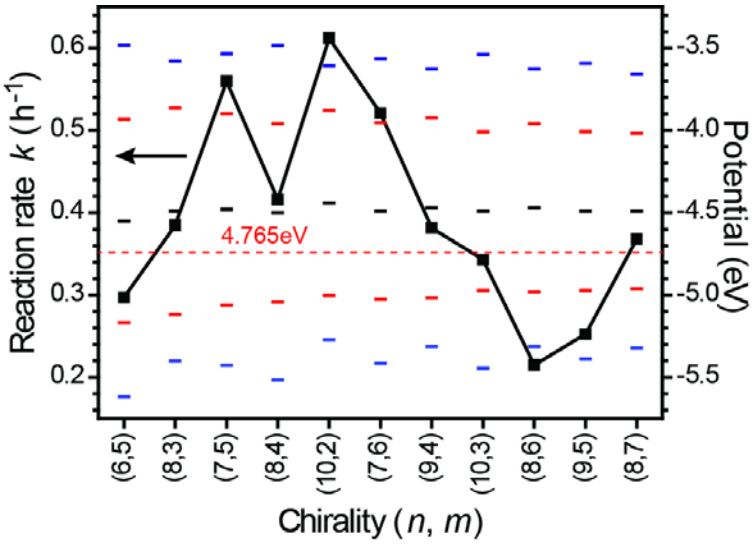

Fig. S7. Overlap plot of chirality-dependent optical transitions and covalent reaction rate k_2 of FMN-SWNT (black squre). Black, red, and blue bars denote Fermi level, the first transition, and the second transition of semiconducting carbon nanotubes, respectively. Chirality-dependent reaction rate was obtained from Figure 5C. The position of the nanotube Fermi level and its optical transitions were obtained from ref. S2 and S3, respectively. Red dashed line indicates reduction potential of 4-MBD.

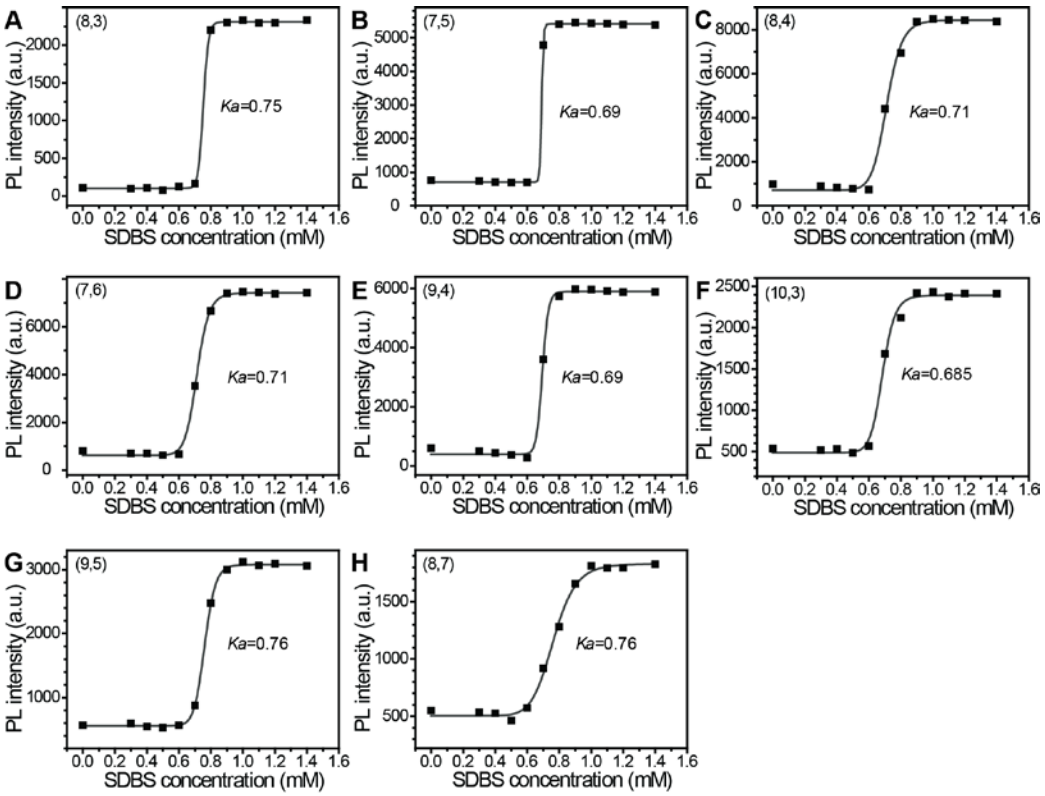

Fig. S8. PL intensities profiles of SWNTs-wrapped with SDBS from the FMN-SWNTs titrated with increasing concentration of SDBS. The Binding affinity (K_a) of FMN-SWNTs determined by PL-based SDBS titration. Curves were fitted using the Hill equation.

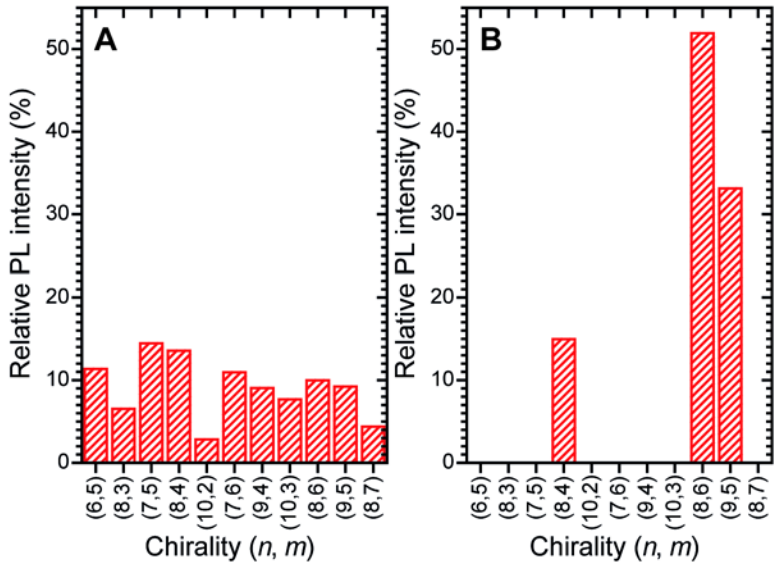

Fig. S9. Relative PL intensity-based population of FMN-wrapped nanotube chirality from (A) before, and (B) after 29 h of the addition of 0.3 mM 4-MBD.

Table S1. Reaction rate (*k*) of FMN-SWNT based on absorption bleaching upon the addition of 0.1 mM 4-MBD.

Optical transitions	Wavelength (nm)	Reaction rate *k* (h^{-1})	Suggested chiralities	
E_{11}^{M}	560	0.37	(8,8), (9,6), (10,4), (11,2)	
	600	0.44	(10,7), (11,5), (12,3), (13,1)	
E_{22}^{S}	659	0.31	(7,5), (7,6), (8,3), (10,3)	
	743	0.35	(10,2), (9,4), (8,6), (8,7)	
	813	0.28	(12,1), (11,1), (10,5), (9,7)	
	874	0.38	(13,3), (12,5), (11,7), (11,9)	
Average reaction rate of E_{11}^{M} transitions (h^{-1})		**0.41**	Average reaction rate of E_{22}^{S} transitions (h^{-1})	**0.33**

Table S2. Chirality assignment of radial breathing mode (RBM) peaks of Figure 3 and their intensity ratio before and after functionalization of FMN-SWNT. *M* and *S* denote metallic and semiconducting nanotubes, respectively.

ω_{RBM} [cm^{-1}]	FWHM [cm^{-1}]	Diameter [nm]	Chirality assignment	Electronic type	Intensity ratio normalized by intensity of (9,2) tube after covalent functionalization
169	12	1.30	(14,4)	*S*	0.47
184	15	1.28	(15,2)	*S*	0.70
213	11	1.15	(8,8)	*M*	0.75
225	7	1.09	(9,6)	*M*	0.24
235	12	1.04	(10,4)	*M*	0.47
243	6	1.01	(11,2)	*M*	0.56
259	7	0.94	(9,3)	*M*	0.84
268	9	0.91	(10,1)	*M*	0.48
286	10	0.85	(9,2)	*S*	1
Average intensity ratio of metallic tubes: **0.56**				Average intensity ratio of semiconducting tubes: **0.72**	

Table S3. As-obtained and FMN-corrected atomic percentages of SWNTs by XPS from before and after covalent functionalization with 0.1 mM 4-MBD for 24 hr.

Functionalization	Atomic %			Subtraction of FMN contribution →	Corrected atomic %	
	C	O	N		C	O
Before	86	9.35	2.2		94.6	5.4
After	76.4	14.9	5.2		94.4	5.6

Table S4. Reaction rate (*k*) of SDS-SWNT based on absorption bleaching upon the addition of 0.1 mM 4-MBD.

Optical transitions	Wavelength (nm)	Reaction rate *k* (h^{-1})	Suggested chiralities	
E_{11}^{M}	554	116.2	(8,8), (9,6), (10,4), (11,2)	
	593	99.6	(10,7), (11,5), (12,3), (13,1)	
E_{22}^{S}	649	48.7	(7,5), (7,6), (8,3), (10,3)	
	726	54.8	(10,2), (9,4), (8,6), (8,7)	
	800	72.4	(12,1), (11,1), (10,5), (9,7)	
	867	92.4	(13,3), (12,5), (11,7), (11,9)	
Average reaction rate of E_{11}^{M} transitions (h^{-1})		**107.9**	Average reaction rate of E_{22}^{S} transitions (h^{-1})	**67.1**

Table S5. Reaction rate *k* based on slow photoluminescence decay fitting of FMN-wrapped SWNTs using 0.1 mM of 4-MBD.

Assignment (*n*,*m*)	Diameter d_t (nm)	Reaction rate *k* (h^{-1})	Assignment (*n*,*m*)	Diameter d_t (nm)	Reaction rate *k* (h^{-1})
(6,5)	0.76	0.30	(9,4)	0.92	0.38
(8,3)	0.78	0.39	(10,3)	0.9	0.34
(7,5)	0.83	0.56	(8,6)	0.97	0.22
(8,4)	0.84	0.42	(9,5)	0.98	0.25
(10,2)	0.88	0.61	(8,7)	1.03	0.37
(7,6)	0.89	0.52	Average reaction rate (h^{-1})		**0.40**

Table S6. Binding affinity (K_a) of FMN-wrapped SWNTs determined by PL-based SDBS titration.

Assignment (*n*,*m*)	Diameter (nm)	Binding affinity (K_a)
(6,5)	0.76	0.71
(8,3)	0.78	0.75
(7,5)	0.83	0.69
(8,4)	0.84	0.71
(10,2)	0.88	0.64
(7,6)	0.89	0.71
(9,4)	0.92	0.69
(10,3)	0.94	0.685
(8,6)	0.97	0.89
(9,5)	0.98	0.76
(8,7)	1.03	0.76
Average binding affinity		**0.726**

Cited References

(S1) Itkis, M. E.; Perea, D. E.; Niyogi, S.; Rickard, S. M.; Hamon, M. A.; Hu, H.; Zhao, B.; Haddon, R. C., "Purity Evaluation of As-Prepared Single-Walled Carbon Nanotube Soot by Use of Solution-Phase Near-IR Spectroscopy", *Nano Lett.* **2003**, *3*, 309-314.

(S2) Tanaka, Y.; Hirana, Y.; Niidome, Y.; Kato, K.; Saito, S.; Nakashima, N., "Experimentally Determined Redox Potentials of Individual (n,m) Single-Walled Carbon Nanotubes", *Angew. Chem., Int. Ed.* **2009**, *48*, 7655-7659.

(S3) Ju, S.-Y.; Doll, J.; Sharma, I.; Papadimitrakopoulos, F., "Selection of carbon nanotubes with specific chiralities using helical assemblies of flavin mononucleotide", *Nat. Nanotechnol.* **2008**, *3*, 356-362.